# Dynamics of T2G2 Helices in Atactic and Syndiotactic Polystyrene: New Evidence from Dielectric Spectroscopy and FTIR

**ARTICLE** *in* MACROMOLECULES · JUNE 2006

Impact Factor: 5.8 · DOI: 10.1021/ma0606758



**3 AUTHORS**, INCLUDING:

S.J. Picken
Delft University of Technology
**249** PUBLICATIONS **4,059** CITATIONS
SEE PROFILE

Michael Wübbenhorst
University of Leuven
**163** PUBLICATIONS **2,606** CITATIONS
SEE PROFILE

# Dynamics of $T_2G_2$ Helices in Atactic and Syndiotactic Polystyrene: New Evidence from Dielectric Spectroscopy and FTIR

**Veronica Lupaşcu,† Stephen J. Picken,† and Michael Wübbenhorst*,‡**

*Department of Chemical Engineering, Delft University of Technology, Julianalaan 136, 2628 BL Delft, The Netherlands, and Department of Physics and Astronomy, Katholieke Universiteit Leuven, Celestijnenlaan 200D, B-3001 Leuven, Belgium*

*Received March 25, 2006; Revised Manuscript Received May 18, 2006*

ABSTRACT: The local and cooperative dynamics in atactic (a-PS) and syndiotactic (s-PS) polystyrene were studied by broadband dielectric spectroscopy. Besides the known α-relaxation, two additional relaxation processes $\beta_1$ and $\beta_2$ were revealed in various samples of a-PS and s-PS films cast from solvent solutions. These new dynamic processes show Arrhenius behavior, a common activation energy around 80 kJ/mol, and cross the α-relaxation region without merging, indicating a molecular origin being phase-separated from the amorphous PS fraction. By Fourier transform infrared spectroscopy (FTIR) measurements, a clear link between the existence of $T_2G_2$ helix conformation and the occurrence of the $\beta_1$- and $\beta_2$-processes was established. Symmetry arguments and systematic differences in the relaxation parameters between a-PS and s-PS favor the assignment of the fast, $\beta_1$, process to a helix defect mechanism (helix inversion), while the slow mode, $\beta_2$, likely originates from cooperative helix inversion events that would point to spatially organized aggregates of helices, as suggested earlier for PS gels. The occurrence of such solvent-induced structures and their dynamics might have important implication for the interpretation of $T_g$ reductions found in ultrathin PS films.

## 1. Introduction

In the past four decades, atactic PS had been studied by a large number of authors, and it becomes the model system for many research topics and particularly, in the past decade, for research on polymers confinement in ultrathin films.[1−3]

While atactic PS represents a purely amorphous polymer, the two stereoregular variants, isotactic (i-PS) and syndiotactic polystyrene, were extensively studied especially for understanding their crystalline properties. The various methods involved in the studies such as Fourier transform infrared spectroscopy (FTIR),[4−6] X-ray diffraction,[6−11] electron diffraction,[12,13] and solid-state nuclear magnetic resonance[14−16] led to the conclusion that both i-PS and s-PS molecules assume different crystalline forms showing a complicated polymorphism.[4,6,8,10,11,17−24]

The essential feature of s-PS is its ability to form stable crystal structures based on two regular chain conformations: the all-trans, planar zigzag conformation that gives rise to the high-temperature crystalline forms α and $\beta$[10,23,25] and the $T_2G_2$ conformation leading to a helical chain structure contained in the $\delta$ and $\gamma$ forms.[8,10]

Actually, the $\delta$ form is a clathrate structure represented by complexes formed by the solvent molecules[6−8,10,23,25] with the polymer chains existing in a s(2/1)2 $T_2G_2$ helix conformation. This form can be obtained by solution cast method[10,21,26,27] or by solvent vapor sorption by the amorphous polymer.[28,29] FTIR results showed that annealing at 120 °C induced full desorption of the solvent but resulted in an imperfect $\gamma$ form containing many nanopores between the polymer chains of the mesophase. It was concluded that the samples annealed at lower temperature exhibited conformational order, but lack of crystalline regularity and the reorganization from $\delta$ to $\gamma$ form may occur perfectly by annealing at 170 °C indicated by the decrease in the number of micropores.[26]

Because of its lack of stereoregularity, a-PS is believed not to crystallize, and it is considered an amorphous polymer. However, it has been shown by NMR[30] that a-PS usually contains a high fraction of syndiotactic sequences in its molecule, and results obtained with model compounds suggest that a-PS is better described by a prevailing syndiotactic configuration of at least eight aliphatic bonds in the trans conformation.[31] Moreover, studies of the supramolecular structure involved in the gelation mechanism of a-PS combined with studies of a-PS in solution with different solvents showed that this polymer forms the same type of complexes with the solvent molecules as the one known for s-PS.[9,19,32−43]

So far, dielectric relaxations spectroscopy was used in studying a-PS only, and the measurements proved to be difficult due to the weak relaxation strength of a-PS.[2,3,44,45]

In this paper we report the first study, to the best knowledge of the authors, of s-PS using dielectric spectroscopy, and the results are compared with a-PS samples prepared under similar conditions.

The structural evidence for conformational state probed by dielectric spectroscopy is further provided by FTIR.

## 2. Experimental Section

**2.1. Broadband Dielectric Relaxation Spectroscopy (BDRS).** *Sample Preparation*. Atactic polymer was received from Shell (PS, Shell N7000, $M_w$ = 371 000, PDI = 3.3) and was purified by triple precipitation from dichloromethane/methanol. To obtain sheetlike samples for dielectric measurements, the precipitate was heated and compression-molded at 200 °C (sample **D1**, cf. Table 1). The same material was used to prepare a PS sample (**D2**) "doped" with 0.1% of the fluorescent probe DBANS by melt mixing in a batch mixer. More details can be found in ref 46.

Syndiotactic polystyrene was received in highly crystalline form (Polymer Source Inc., $M_w$ = 250 kg/mol). From this material, sheets with a typical thickness between 2 and 10 $\mu$m were prepared by compression-molding at about 270 °C, which were subsequently processed further by three different sample preparation routes. Amorphous samples (**D3**) were obtained by heating the sheets again

† Delft University of Technology.
‡ Katholieke Universiteit Leuven.
* Corresponding author. E-mail: Michael.Wubbenhorst@fys.kuleuven.be.

10.1021/ma0606758 CCC: $33.50 
Published on Web 06/27/2006

**Table 1. Sample Overview**

(a) DRS Samples

| polymer | sample code | $\beta_1/\beta_2$-processes present? | preparation details |
|---|---|---|---|
| a-PS | **D1** | weak/weak | precipitated from DCM solution in methanol, compression-molded at 200 °C |
| a-PS + 0.1% DBANS | **D2** | weak/weak | precipitated from DCM solution in methanol, melt mixing of DBANS at 200 °C, compression-molding at 200 °C[46] |
| s-PS | **D3** | not present | compression-molded at 200 °C, remelted at 270 °C for >1 min, then quenched in ice water |
| s-PS | **D4** | weak/? | compression-molded at 200 °C, remelted at 270 °C for ~10 s, then quenched to RT |
| s-PS | **D5** | strong/strong | spin-cast from $CHCl_3$, annealing at 80 °C for 2 h |

(b) FTIR Samples

| polymer | sample code | solvent | preparation details |
|---|---|---|---|
| a-PS | **F1** | toluene | spin-cast from 5% solution in toluene on KBr crystal window, no annealing |
| s-PS | **F2** | | amorphous s-PS measured as freely standing film (same preparation history as D3) |
| s-PS | **F3** | toluene | 3 days solvent uptake by amorphous sheets, dried for 30 min at 80 °C mixed with KBr powder and prepared as round crystal windows |
| s-PS | **F4** | $CHCl_3$ | 3 days solvent uptake by amorphous sheets, dried for 30 min at 80 °C mixed with KBr powder and prepared as round crystal windows |

above the melting point (270 °C) and subsequently quenching them in ice water. Sample **D4** was prepared in a similar way; however, the sample was kept at 270 °C only for about 10 s, and the cooling rate was slower (quenched on a precooled metal plate at $T = -20$ °C).

For dielectric measurements, samples from the sheet materials **D1**−**D4** were provided with circular-shaped ($D = 2$ cm) electrodes by evaporation of ~50 nm aluminum layer on both sides. After that, samples were clamped between the massive electrodes of a dielectric sample cell and subjected to individual heating and cooling cycles within the temperature range from −120 to 270 °C.

Sample **D5** was prepared in a very different way. A part of the amorphous material (**D3**) was again dissolved in chloroform. Thin films (115 nm) were prepared by spin-coating (at 1000 rpm for 30 s) on aluminum-coated glass slides. After annealing for 2 h at 80 °C, samples were provided with a second electrode by depositing aluminum in a "flash" evaporation process, i.e., ultrafast deposition with the maximum available evaporation rate (>10 nm/s)[47] that ensures both a sharp and smooth polymer/metal interface. The film prepared from solution was measured during heating with a temperature range from −15 to 270 °C.

*Dielectric Measurements and Data Analysis.* Dielectric measurements were performed using a high-precision dielectric analyzer (ALPHA analyzer, Novocontrol Technologies) in combination with a Novocontrol Quatro temperature system providing control of the sample temperature with high stability (<0.05 K). Temperature-dependent experiments were performed by consecutive isothermal frequency sweeps ($10^{-1}$−$10^7$ Hz) in the temperature range from +200 to −120 °C in steps of 5 K, which resulted in an effective (mean) cooling rate of about 0.5 K/min. For an accurate determination of the relaxation time $\tau(T)$ and other relaxation parameters we fitted the dielectric loss spectra $\epsilon''(\omega)$ to the imaginary part of the empirical Havriliak−Negami (HN) relaxation function (eq 1):[46]

$$\epsilon'' = -\mathrm{Im}\left\{\frac{\Delta\epsilon}{(1+(i\omega\tau)^a)^b}\right\} + \frac{\sigma}{\epsilon_v\omega} \qquad (1)$$

where $\Delta\epsilon$ corresponds to the relaxation strength, while the two "shape parameters" $a$ and $b$ represent the logarithmic slope of the low-frequency loss tail ($a$) and the high-frequency loss tail ($-ab$). The second term in eq 1 accounts for Ohmic conduction.

A comprehensive description of analysis methods for dielectric data can be found in the refs 48 and 49.

**2.2. Fourier Transform Infrared Spectroscopy (FTIR).** *Sample Preparation and FTIR Setup.* FTIR measurements were performed on four different samples (cf. Table 1b), which were chosen to match the morphology of the DRS samples (**D1**−**D5**) as much as possible. Amorphous s-PS (**F2**) was prepared in the same way as the DRS equivalent (**D3**) and was measured as a freely standing film. A sample of atactic PS (**F1**) was obtained as follows. A solution of 5 wt % PS in toluene was spin-coated (3000 rpm for 30 s) on KBr round crystal windows (diameter = 25 mm, thickness = 2 mm) and measured after drying at room temperature. For the preparation of these samples, atactic polystyrene (Pressure Chemical Co.) with an intermediate molecular mass ($M_w$ = 160 000 g/mol) and low polydispersity (<1.06) was used.

To compare the helix formation in both syndioactic and atactic PS, two other samples were prepared as follows: very small (couple of millimeters in diameter) fragments from the amorphous sheets of syndiotactic PS were immersed in two different solvents: toluene (sample **F3**) and chloroform (sample **F4**). At room temperature none of the solvents dissolves the polymer completely; however, it is known from the literature that the solvent uptake is sufficient to promote the coil to helix transformation of the polymer chains inside the swollen PS sheets.[28,29]

After 3 days, the s-PS sheets were taken out of the solvent and were dried for 30 min at 80 °C, subsequently mixed with KBr powder, and prepared as round crystal windows by means of a hydraulic press.

For the FTIR measurements a Perkin-Elmer Spectrum One FTIR spectrometer was used in single-beam mode. Data were collected over a range of 4000−450 $cm^{-1}$ with a resolution of 0.5 $cm^{-1}$.

## 3. Results

**3.1. Dielectric Relaxations.** Dielectric relaxation spectroscopy was applied to study the molecular dynamics of the various PS samples in a wide temperature range covering the glassy, semicrystalline, or amorphous liquid state. Figure 1 shows a 3D representation of the dielectric loss $\epsilon''_{deriv}(f,T)$ of a-PS sample (**D1**). Like in previous work,[48,50,51] we have used the "conduction-free" dielectric loss ($\epsilon''_{deriv}$), computed from the real part of the dielectric spectrum $\epsilon'(f)$,[48] in order to eliminate excessive contributions from (Ohmic) conduction in the loss spectra.[52−54] The resulting "loss" $\epsilon''_{deriv}(f,T)$ spectra reveal the dominant main α relaxation process, well-known from the literature,[55] as well as a second process that "passes" the α-process at about

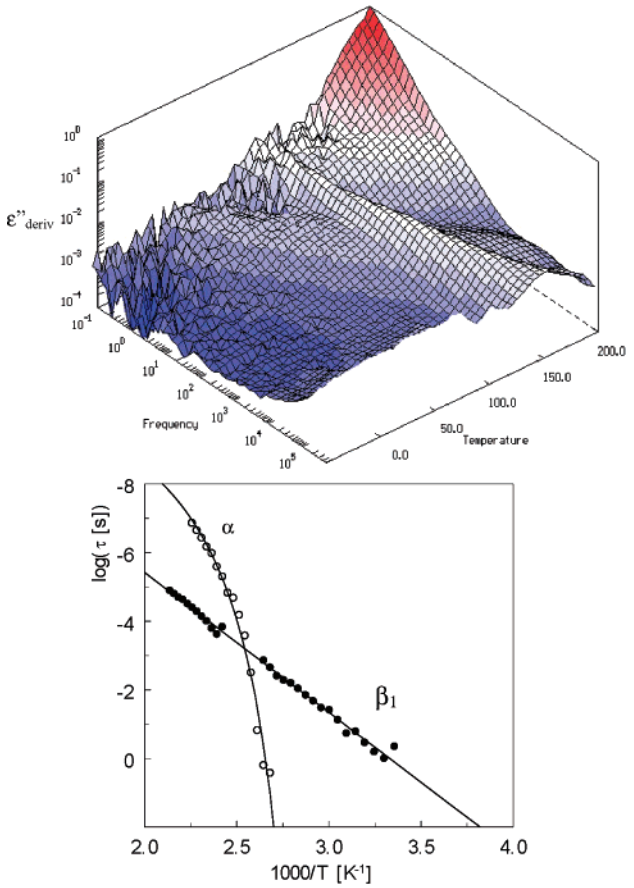


**Figure 1.** First observation of an additional high-temperature Arrhenius process ($\beta_1$-process) in a-PS (**D1**). Top: three-dimensional representation of the "conduction-free" dielectric loss $\epsilon''_{deriv}(f,T)$. Bottom: activation plot log($\tau$) vs inverse temperature.

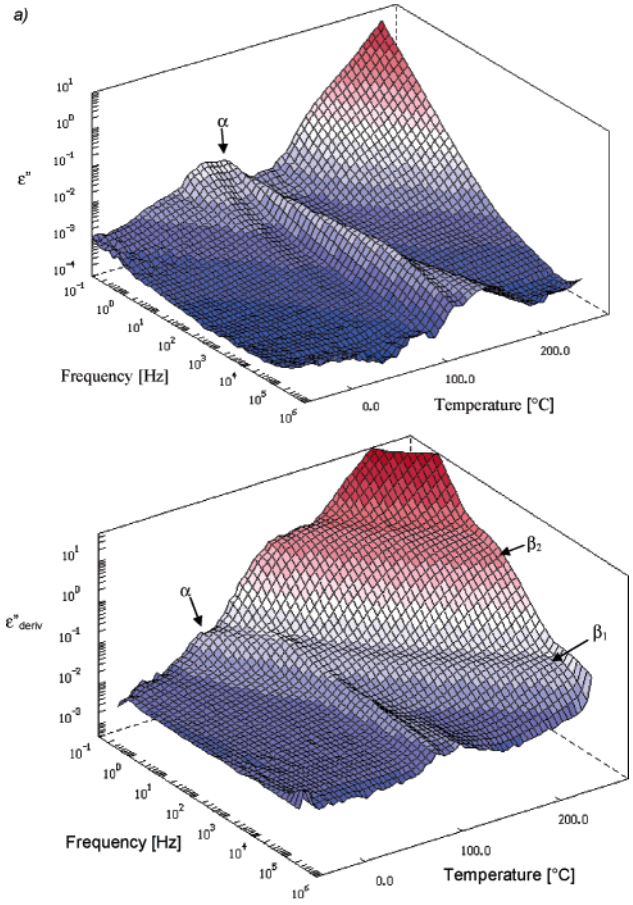


**Figure 2.** Three-dimensional representation of the "conduction-free" dielectric loss $\epsilon''_{deriv}(f,T)$ for two differently prepared samples of s-PS: (a) amorphous sample **D3**; (b) cast sample (**D5**) from $CHCl_3$ solution.

100 Hz. This peculiar effect, the coexistence of two crossing, obviously independent dynamic processes, is also seen in the activation plot (Figure 1b).

The α-relaxation is generally attributed to the dielectric manifestation of the dynamic glass transition, and such a relaxation process crossing the α-relaxation has not been reported for a-PS previously. Instead, below the glass transition temperature, three other relaxation processes have been described in the literature, which were assigned to local molecular motions, some of them related to specific structural features of the polymer chain: around 50 °C ($f = 100$ Hz), occasionally a $\beta$ process[55] has been observed for a-PS having bulky substitutes at the chain ends or for a-PS with very low molecular mass. At much lower temperatures (−120 °C at $f = 100$ Hz), the $\gamma$ relaxation shows up, which has been assigned to local motions involving head-to-head irregularities in the polymer chain.[55] Sinnott at al. reported an additional ($\delta$) process located around 40 K[56] and attributed this to phenyl group motions.

To assign the new relaxation mode, which we further refer to as the $\beta_1$-process, and since it is obvious that the relaxation behavior of polystyrene is very sensitive to the microstructure, particularly the stereoregularity, we studied syndiotactic PS for comparison. Although s-PS was extensively investigated regarding its complex phase behavior and morphology, no measurements of the dielectric relaxation dynamics have been reported yet.

An illustration of this complex phase behavior of s-PS is given by Figure 2, which displays the dielectric loss data of a fully amorphous sample **D3** (Figure 2a), in comparison with the sample **D5** prepared from $CHCl_3$ solution (Figure 2b). While the amorphous sample **D3** reveals a single relaxation process (α), the solvent prepared sample **D5** exhibits two additional relaxation modes, the fast one of which resembles the previously described $\beta_1$-relaxation. Despite this difference, both samples show crystallization upon heating at ∼120 °C, indicated by the discontinuous change in the α-relaxation peak at this temperature. Interestingly, this crystallization affects the α-process in the same way for the two samples without interfering with the $\beta_1$-relaxation in **D5**. The strong dielectric dispersion of sample **D3** just below $T_g$ is due to the strong nonequilibrium state of the sample after quenching, an effect that vanishes immediately after passing the "equilibrium" $T_g$.

For comparison of the relaxation behavior of a-PS and s-PS, the dielectric loss spectra of various samples measured at 150 °C are displayed in Figure 3. Three dielectric processes can be distinguished, though some differences exist in the strength of the individual relaxation processes. The α-process visible around $f = 100$ kHz is present for all samples. In the medium-frequency range (100−1000 Hz), the $\beta_1$-relaxation can be seen for all samples except for the amorphous sample containing s-PS (**D3**). At low frequencies, a third relaxation mode ($\beta_2$) shows up, which is missing as well for sample **D3**. Despite the variation in the peak intensity among the different samples, we can note that both new $\beta$-processes have a generally narrow peak width, which is not typical for common secondary relaxations in polymers.

To determine the detailed relaxation parameters including the thermal activation parameters, the dielectric data were analyzed by fitting isothermal spectra $\epsilon''(f)$ to eq 1, which yielded the temperature dependence of the relaxation time $\tau(T)$ and the other

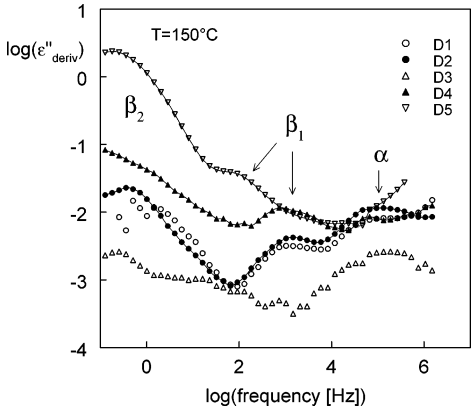


**Figure 3.** Dielectric loss spectrum $\epsilon''_{deriv}(f)$ at $T = 150$ °C for various samples of atactic and syndiotactic PS: **D1** (a-PS compression-molded at 200 °C) (○), **D2** (a-PS compression-molded at 200 °C + DBANS) (●), **D3** (amorphous s-PS, fast quenched) (△), **D4** (s-PS slow quenched) (▲), and **D5** (s-PS solvent prepared) (▽).

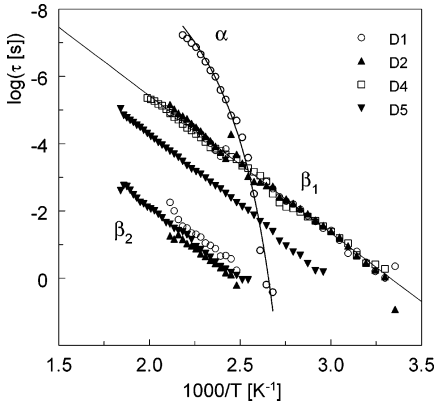


**Figure 4.** Activation diagram showing the peak relaxation times $\tau_{\beta_1}$ and $\tau_{\beta_2}$ for four various PS samples: **D1** (a-PS compression-molded at 200 °C) (○), **D2** (a-PS compression-molded at 200 °C + DBANS) (▲), **D4** (s-PS quenched slow) (□), and **D5** (s-PS solvent prepared) (▼).

HN parameters of each relaxation process. The relaxation time data are plotted in the Arrhenius diagram shown in Figure 4. As expected, the α-process, characterized by its typical curvature in the temperature dependence of the relaxation time, $\tau(T)$, can be fitted to the VFT law

$$\tau = \tau_\infty \exp\left(\frac{E_V}{R(T - T_V)}\right) \quad (2)$$

where $E_V$ and $T_V$ are the "Vogel activation energy" and the Vogel temperature.[57−59] The other two parameters $R$ and $\tau_\infty$ have the usual meaning.

In contrast, all the other data obey the Arrhenius equation (eq 3) being indicative for "simple" thermally activated behavior:

$$\tau = \tau_\infty \exp\left(\frac{E_a}{RT}\right) \quad (3)$$

The activation parameters $E_a$ and $\log(\tau_\infty)$ for all samples and processes are listed in Table 3. From Figure 4 we see that all relaxation data $\tau(T)$ have virtually the same slope, indicating an unique activation energy around 80 kJ/mol. For the slow $\beta_2$-process, there is only little dependence of the relaxation time on the sample material; i.e., the $\beta_2$-relaxation shows no sensitivity to the tacticity of the polymer. The relaxation time values for the $\beta_1$-relaxation reveal similar behavior though shifted in frequency by about 3 decades. Again, most of the

**Table 2. Various IR Absorption Bands of Ring, Amorphous, and $T_2G_2$ Modes According to the Literature**

| wavenumber ($cm^{-1}$) | system | assignment | ref |
|---|---|---|---|
| 502 | s-PS | $T_2G_2$ | 28 |
| 535 | s-PS/$CCl_3$ | $T_2G_2$ | 62 |
| 541 | s-PS/$CCl_3$ | amorphous | 62 |
| 548 | s-PS/$CCl_3$ | $T_2G_2$, $m = 7-12$ | 62 |
| 571 | s-PS/$CCl_3$ | $T_2G_2$, $m = 20-30$ | 62 |
| | a-PS/$CS_2$ | | 41 |
| 1069 | s-PS/$CCl_3$ | ring mode of s-PS | 62 |

$\tau_{\beta_1}(T)$ data from a-PS and s-PS (**D1**, **D2**, **D4**) show a unique behavior within the experimental error, the only exception being sample **D5**, which we will discuss later in this paper.

The relaxation strength $\Delta\epsilon(T)$ of the $\beta_1$ and $\beta_2$ relaxation as a function of the temperature for four different PS samples is presented in Figure 5. The two processes have about the same relaxation strength with values ranging between 0.01 and 0.08. However, there is an exception presented by the relaxation strength of the $\beta_2$-process of the sample **D5** (syndiotactic PS cast from chloroform), which is much higher compared with the other samples. For this particular sample the *y*-axis indicated in Figure 5 by the arrow is depicted on the right side of the graph.

It is clearly seen that the strongest $\beta_1$- and $\beta_2$-processes belong to the sample **D5,** which contains solvent prepared syndiotactic PS, while the samples **D1** and **D2** show the weakest processes.

The relaxation strength for the $\beta_1$-process ($\Delta\epsilon_{\beta_1}$) shows a slight decrease with the increasing temperature for all samples presented. Relaxation strength values for the $\beta_2$-process ($\Delta\epsilon_{\beta_2}$), though being a bit more scattered, reveal the same type of temperature dependence for the sample **D5**, while for samples **D1** and **D2** a reverse trend can be noticed.

**3.2. FT-IR Spectra.** The existence of specific molecular conformations of the polymer chains inside the films prepared from solvent solutions is confirmed by FTIR measurements. It is well-known that the infrared spectrum of s-PS is very sensitive to the local conformations of the chains.[60,61] FTIR spectra contain absorption bands that are specific to both $T_2G_2$ and TTTT conformations, while other bands (ring modes) show no conformation sensitivity and thus provide an internal reference. A summary of some relevant IR absorption bands and their assignment is given in Table 2.

Figure 6 presents the normalized mid-infrared (MIR) FTIR absorption spectra of four PS samples. The samples used in this experiment, their name, and preparation procedure are listed in Table 1b.

Within the spectral region from 500 to 600 $cm^{-1}$ a broad peak with a maximum at 540 $cm^{-1}$ is seen that is characteristic of the amorphous part of the polymer here measured for the sample **F2**. Sample **F2** (amorphous syndiotactic PS) has the same preparation history as the sample **D3**. Some of the characteristic infrared bands of PS are influenced by the type of conformation as well as by its sequential length *m* (number of monomer units they contain), and the sensitivity to the length of a particular conformation differs from band to band. The bands in the 500−600 $cm^{-1}$ region are due to out of plan deformation of the phenyl ring, and they are conformational sensitive to the $T_2G_2$ helix sequences.[41,62] For comparison, two solvent prepared s-PS samples **F3** and **F4** were measured, and the spectra are shown in Figure 6 by interrupted lines. Here the strong peak at 540 $cm^{-1}$, characteristic of a random conformation, is absent, and two new absorption peaks at 535 and 548 $cm^{-1}$ being indicative for the $T_2G_2$ helix conformation are clearly visible. Chloroform and toluene were chosen as solvents,

**Table 3. Activation Parameters for the $\beta_1$- and $\beta_2$-Relaxations Found in a-PS and s-PS**

| | | $\beta_1$-process | | | $\beta_2$-process | | | |
|---|---|---|---|---|---|---|---|---|
| sample | | $E_A$ [kJ/mol] | log ($\tau_\infty$ [s]) | $\Delta\epsilon$ (150 °C) | $E_A$ [kJ/mol] | log ($\tau_\infty$ [s]) | $\Delta\epsilon$ (150 °C) | $\Delta\epsilon_{\beta_2}/\Delta\epsilon_{\beta_1}$ |
| a-PS | **D1** | $79 \pm 2$ | $-13.7 \pm 0.4$ | $0.012 \pm 0.001$ | $76 \pm 2$ | $-10.2 \pm 0.5$ | $0.027 \pm 0.002$ | 2.4 |
| a-PS + 0.1% DBANS | **D2** | $83 \pm 2$ | $-14.3 \pm 0.4$ | $0.013 \pm 0.001$ | $78 \pm 2$ | $-10.0 \pm 0.5$ | $0.050 \pm 0.003$ | 4.0 |
| s-PS | **D3** | | | | | | | |
| s-PS | **D4** | $77 \pm 2$ | $-13.4 \pm 0.4$ | $0.030 \pm 0.002$ | | | | |
| s-PS | **D5** | $82 \pm 2$ | $-12.9 \pm 0.4$ | $0.065 \pm 0.004$ | $83 \pm 2$ | $-10.7 \pm 0.5$ | $2.6 \pm 0.1$ | 40.2 |

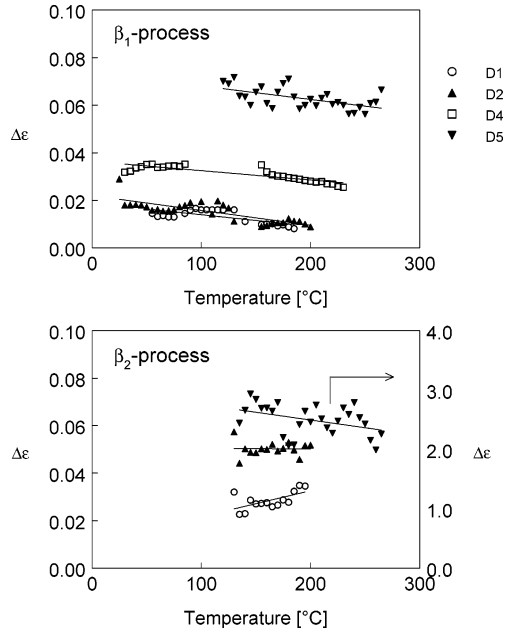


**Figure 5.** Relaxation strength $\Delta\epsilon(T)$ of the $\beta_1$- and $\beta_2$-relaxation as a function of the temperature for four different PS samples: **D1**(a-PS compression-molded at 200 °C) (○), **D2** (a-PS compression-molded at 200 °C + DBANS) (▲), **D4** (s-PS quenched slow) (□), and **D5** (s-PS solvent prepared) (▼).

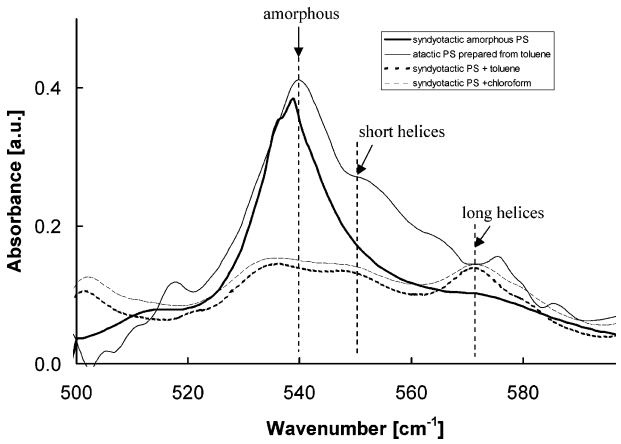


**Figure 6.** Normalized MIR FTIR of four samples of PS: details about the samples are given in the figure caption.

and there are no visible differences between the two spectra in the region presented.

Table 2 presents the corresponding length of the helices to the specific infrared bands in this region.

The last spectrum in Figure 6, depicted by a thin continuous line, represents the IR response from the sample $\mathbf{F}_1$, atactic PS prepared from toluene. The two peaks at 548 and 572 $cm^{-1}$ known to be characteristic of helix conformation for both a-PS and s-PS appear in the spectrum as pronounced shoulders to the broad amorphous peak (540 $cm^{-1}$).[41,62] These particular peaks are absent in an amorphous sample (not presented in this paper) of pure a-PS. From Figure 6 it is clear that populations of long and short helices are present in all samples.

## 4. Discussion

The discovery of two, yet unknown relaxation processes in polystyrene, a polymer that is well established as both engineering material and as a model system in polymer science, is somewhat surprising. There are some possible explanations for the fact that these processes where not reported previously. First of all, the dielectric losses in PS are generally low compared to other, well-studied polar polymers, and this has hampered broad systematic studies on such a low-loss system in the past. Furthermore, to reveal the very slow $\beta_2$-process unambiguously, advanced fit strategies or the alternative $\epsilon''_{deriv}$ technique are necessary to eliminate strong loss contributions due to Ohmic conductivity.

Second, syndiotactic PS would have been a better candidate to detect these relaxation modes due to the higher strength of the $\beta_1$- and $\beta_2$-processes in this polymer. However, no DRS study has been reported so far on s-PS despite the large number of publications on this material in the last years, though a recent paper by d'Aniello et al.[63] showed that dynamic-mechanical measurements are sensitive to polymorphic phase transitions-($\alpha$, $\gamma$, $\delta$, and clathrate) of s-PS.

The third but not less important explanation is that the results so far show that the $\beta_1$- and $\beta_2$-processes were exclusively found in samples that have a solvent history. Melt prepared samples from both s-PS, **D3** in this study, and a-PS, not presented here, show no such processes, which led us to the conclusion that the two processes are indicative for specific solvent-induced structures.

In view of the rich literature dealing with conformation transitions from coil to helix (rod) in solutions of s-PS and a-PS, together with spectroscopic evidence from FTIR (cf. Figure 6), it is quite evident that the new dielectric relaxation processes are related to the existence of helical structures involving syndiotactic sequences.[34,35,41,60] To identify the molecular mechanism that links the specific dielectric relaxations $\beta_1$ and $\beta_2$ to the conformational regular, helical structure, we have to revisit the main finding from the previous section: (1) Though the relaxation strength for the $\beta_1$- and $\beta_2$-processes is slightly different for a-PS and s-PS, the fact that they have the same activation energy points to a common inter- or intramolecular potential involved in both fluctuations. (2) The ultimate higher relaxation strengths found for the syndiotactic samples are in line with a potentially larger volume fraction of helical sequences in s-PS than in a-PS. (3) For a given microstructure, expressed by the tacticity, a systematic variation of preparation conditions allows the variation of the helical fraction, and this can be seen from the relaxation strength variation for different samples presented in this paper in Figure 5.

The assignment of the two dielectric relaxation modes to specific fluctuations of helical rods is less straightforward. Fluctuations of entire helices around the long axis (rotations) of the short axis (librations) should not have a manifestation as a dielectric relaxation process since $T_2G_2$ helices exhibit neither

a net longitudinal or transversal dipole moment, for symmetry reasons. Consequently, the observed dynamic processes must be related to a well-defined defect mechanism being an intrinsic feature of helical structures. Such a plausible mechanism is the *helix inversion* which takes plays at the interconnection between left-handed and right-handed PS-helices and which has been described in detail by Brückner et al.[64]

The dynamics of *kink* (*or helix*) *inversion* is likely responsible for the fast process, which sets in at temperatures much lower than the glass transition temperature. Compared to the $\beta_1$-process, the $\beta_2$-relaxation is stronger and slower by roughly 3 decades. Nevertheless, it shows virtually the same activation energy. Both features of the $\beta_2$-process imply a cooperative nature of this slow dynamic process, which might be rationalized by "concerted" helix inversions as being a plausible process in 3-dimensional aggregates of helical rods. It should be noted that, in our experiments, the helical structures reveal enormous stability even when annealing the samples up to the melting temperature (270 °C) of the all-trans crystalline phase. This can be explained by the fact that, on one hand, our samples are not annealed for long enough periods of time at this temperature to completely eliminate the helices formed by parts of the polymer chains inside the film and, on the other hand, the samples are measured in a sandwich configuration where the polymer film is clamped between two aluminum electrodes. This type of sample geometry might hamper the complete transformation of polymer chains into the all-trans conformation being characteristic of s-PS at very high temperatures, and parts of the helices are still maintained after cooling.

We think that these new, solvent-induced, structures and their dynamics have important implication for the interpretation of $T_g$ reductions found in ultrathin PS film, an issue that will be the subject of a forthcoming publication.

## 5. Conclusions

Using dielectric relaxation spectroscopy, two relaxation processes $\beta_1$ and $\beta_2$ not reported before in the literature were revealed in both a-PS and s-PS. These new dynamic processes show Arrhenius behavior and a common activation energy around 80 kJ/mol, and they cross the α-relaxation region without merging, indicating the coexisting of an amorphous together with a nonamorphous phase with specific structural and dynamic properties.

The $\beta_1$- and $\beta_2$-processes are dielectric manifestations of local fluctuations within helical "rods" formed by syndiotactic sequences, which are present in both atactic and s-PS. While the fast relaxation mode assigned to a defect mechanism (helix inversion), the presence of the slow process indicates the existence of helical aggregates as suggested earlier for PS gels.

The clear link between fraction of $T_2G_2$ conformation and the strength of relaxation processes supports assignment of the two relaxation processes to molecular fluctuations involving helical moieties.

In this tentative picture, relaxation details of the $\beta_2$-process might contain information about packing details of helices in the $\delta$ or $\gamma$ phase, which turn out to exhibit an exceptional temperature stability even above the melting temperature of the high-temperature crystalline phase.

By FTIR measurements, a clear link between the existence of $T_2G_2$ helix conformation and the occurrence of the $\beta_1$- and $\beta_2$-processes was established.

The general observation of the $\beta_1$- and $\beta_2$-relaxations in all solvent prepared samples (regardless of the solvent used) further implies that the existence of helical rods and helical aggregates is likely a general issue for PS samples obtained by spin-coating, and further consideration is needed in all studies dealing with solvent prepared PS samples.

**Acknowledgment.** Veronica Lupaşcu gratefully acknowledges the Dutch Organization for Fundamental Research on Matter (FOM) for funding this research project, Piet Droppert for his lab assistance, and Otto van der Berg for his valuable help with the preparation of s-PS samples.

## References and Notes

(1) Keddie, J. L.; Jones, R. A. L.; Cory, R. A. *Europhys. Lett.* **1994**, *27*, 59.
(2) Fukao, K.; Miyamoto, Y. *Phys. Rev. E* **2000**, *61*, 1743.
(3) Lupascu, V.; Huth, H.; Schick, C.; Wubbenhorst, M. *Thermochim. Acta* **2005**, *432*, 222.
(4) Kobayashi, M.; Nakaoki, T.; Ishihara, N. *Macromolecules* **1989**, *22*, 4377.
(5) Kobayashi, M.; Nakaoki, T.; Ishihara, N. *Macromolecules* **1990**, *23*, 78.
(6) Guerra, G.; Manfredi, C.; Musto, P.; Tavone, S. *Macromolecules* **1998**, *31*, 1329.
(7) De Rosa, C.; Rapacciuolo, M.; Guerra, G.; Petraccone, V.; Corradini, P. *Polymer* **1992**, *33*, 1423.
(8) De Rosa, C.; Guerra, G.; Petraccone, V.; Pirozzi, B. *Macromolecules* **1997**, *30*, 4147.
(9) Vittoria, V.; de Candia, F.; Ianelli, P.; Immirzi, A. *Makromol. Chem., Rapid Commun.* **1988**, *9*, 765.
(10) Chatani, Y.; Shimane, Y.; Inoue, Y.; Inagaki, T.; Ishioka, T.; Ijitsu, T.; Yukinari, T. *Polymer* **1992**, *33*, 488.
(11) De Rudder, J.; Berge, B.; Berghmans, H. *Macromol. Chem. Phys.* **2002**, *203*, 2083.
(12) Greis, O.; Xu, Y.; Asano, T.; Petermann, J. *Polymer* **1989**, *30*, 590.
(13) Pradere, P.; Thomas, E. L. *Macromolecules* **1990**, *23*, 4954.
(14) Grassi, A.; Longo, P.; Guerra, G. *Makromol. Chem., Rapid Commun.* **1989**, *10*, 687.
(15) Gomez, M. A.; Tonelli, A. E. *Macromolecules* **1990**, *23*, 3385.
(16) Capitani, D.; De Rosa, C.; Ferrando, A.; Grassi, A.; Segre, A. L. *Macromolecules* **1992**, *25*, 3874.
(17) Nakaoki, T.; Kobayashi, M. *J. Mol. Struct.* **1991**, *242*, 315.
(18) Daniel, C.; Deluca, M. D.; Guenet, J.-M.; Brulet, A.; Menelle, A. *Polymer* **1996**, *37*, 1273.
(19) Daniel, C.; Menellet, A.; Brulett, A.; Guenet, J. M. *Polymer* **1997**, *38*, 4193.
(20) Musto, P.; Manzari, M.; Guerra, G. *Macromolecules* **2000**, *33*, 143.
(21) Amutha, D. R.; Yamato, Y.; Saito, A.; Sivakumar, M.; Tsujita, Y.; Yoshimizu, H.; Kinoshita, T. *J. Polym. Sci., Part B: Polym. Phys.* **2002**, *40*, 530.
(22) Mohri, S.; Rani, D. A.; Yamamoto, Y.; Tsujita, Y.; Yoshimizu, H. *J. Polym. Sci., Part B: Polym. Phys.* **2004**, *42*, 238.
(23) Chatani, Y.; Shimane, Y.; Ijitsu, T.; Yukinari, T. *Polymer* **1993**, *34*, 1625.
(24) Guerra, G.; Vincenzo, M. V.; De Rosa, C.; Petraccone, V.; Corradini, P. *Macromolecules* **1990**, *23*, 1539.
(25) Guerra, G.; Vincenzo, M. V.; De Rosa, C.; Petraccone, V.; Corradini, P. *Macromolecules* **1990**, *23*, 1539.
(26) Tsutsui, K.; Tsujita, Y.; Yoshimizu, H.; Kinoshita, T. *Polymer* **1998**, *39*, 5177.
(27) Rizzo, P.; Lamberti, M.; Albunia, A. R.; de Ballesteros, O. R.; Guerra, G. *Macromolecules* **2002**, *35*, 5854.
(28) Tashiro, K.; Ueno, Y.; Yoshioka, A.; Kobayashi, M. *Macromolecules* **2001**, *34*, 310.
(29) Tashiro, K.; Yoshioka, A. *Macromolecules* **2002**, *35*, 410.
(30) Bovey, F. A.; Hood, F. P.; Anderson, E. W.; Snyder, L. C. *J. Chem. Phys.* **1965**, *42*, 3900.
(31) Jasse, B.; Monnerie, L. *J. Mol. Struct.* **1977**, *39*, 165.
(32) Jasse, B.; Koenig, J. L. *J. Polym. Sci., Polym. Phys.* **1978**, *16*, 1869.
(33) Gan, J. Y. S.; Francois, J.; Guenet, J.-M. *Macromolecules* **1986**, *19*, 173.
(34) Francois, J.; Gan, J. Y. S.; Guenet, J.-M. *Macromolecules* **1986**, *19*, 2755.
(35) Francois, J.; Gan, J.; Sarazin, D.; Guenet, J.-M. *Polymer* **1988**, *29*, 898.
(36) Tanaka, K.; Matsuyama, A. *Phys. Rev. Lett.* **1989**, *62*, 2759.
(37) Xie, M. X.; Tanioka, A.; Miyasaka, K. *Polymer* **1992**, *34*, 1388.
(38) Izumi, Y.; Katano, S.; Funahashi, S.; Furusaka, M.; Arai, M. *Physica B* **1992**, *180&181*, 539.
(39) Izumi, Y.; Kanaya, T.; Shibata, K.; Inoue, K. *Physica B* **1992**, *180&181*, 542.

(40) Izumi, Y.; Katano, S.; Funahashi, S.; Furusaka, M.; Arai, M. *Physica B* **1992**, *180&181*, 545.
(41) Yanxiang, W.; Deyan, S. *Polym. Bull. (Berlin)* **1997**, *39*, 633.
(42) van Hooy-Corstjens, C. S. J.; Magusin, P. C. M. M.; Rastogi, S.; Lemstra, P. J. *Macromolecules* **2002**, *35*, 6630.
(43) De Rudder, J.; Berghmans, H.; De Schryver, F. C.; Bosco, M.; Paoletti, S. *Macromolecules* **2002**, *35*, 9529.
(44) Fukao, K.; Miyamoto, Y. *Phys. Rev. E* **2001**, *6401*, 1803.
(45) Fukao, K.; Uno, S. B.; Miyamoto, Y.; Hoshino, A.; Miyaji, H. *J. Non-Cryst. Solids* **2002**, *307*, 517.
(46) van den Berg, O.; Sengers, W. G. F.; Jager, W. F.; Picken, S. J.; Wübbenhorst, M. *Macromolecules* **2004**, *37*, 2460.
(47) Strunskus, V. Z. T.; Behnke, K.; Bechtolsheim, C. v.; Faupel, F. *Adv. Eng. Mater.* **2000**, *2*, 489.
(48) Wübbenhorst, M.; van Turnhout, J. *J. Non-Cryst. Solids* **2002**, *305*, 40.
(49) van Turnhout, J.; Wübbenhorst, M. *J. Non-Cryst. Solids* **2002**, *305*, 50.
(50) Smits, A. L. M.; Wübbenhorst, M.; Kruiskamp, P. H.; van Soest, J. J. G.; Vliegenthart, J. F. G.; van Turnhout, J. *J. Phys. Chem. B* **2001**, *105*, 5630.
(51) Wübbenhorst, M.; van Koten, E.; Jansen, J.; Mijs, M.; van Turnhout, J. *Macromol. Rapid Commun.* **1997**, *18*, 139.
(52) Hilfer, R. *Phys. Rev. B* **1991**, *44*, 60.
(53) Hartmann, L.; Gorbatschow, W.; Hauwede, J.; Kremer, F. *Eur. Phys. J. E* **2002**, *8*, 145.
(54) Bona, N.; Ortenzi, A.; Capaccioli, S. *J. Pet. Sci. Eng.* **2002**, *33*, 87.
(55) McCrum, N. G.; Read, B. E.; Williams, G. **1967**.
(56) Sinnott, K. M. *SPE Trans.* **1962**, 65.
(57) Vogel, H. *Z. Phys.* **1921**, *22*, 645.
(58) Fulcher, G. S. *J. Am. Ceram. Soc.* **1925**, *8*, 339.
(59) Tamman, G.; Hesse, G. *Z. Anorg. Alleg. Chem.* **1926**, *156*, 245.
(60) Albunia, A. R.; Musto, P.; Guerra, G. *Polymer* **2006**, *47*, 234.
(61) Amutha, D. R.; Yamato, Y.; Saito, A.; Sivakumar, M.; Tsujita, Y.; Yoshimizu, H.; Kinoshita, T. *J. Polym. Sci., Part B: Polym. Phys.* **2002**, *40*, 530−536.
(62) Uda, F.; Kaneko, F.; Kawaguchi, T. *Polymer* **2004**, *45*, 2221.
(63) D'Aniello, C.; Rizzo, P.; Guerra, G. *Polymer* **2005**, *46*, 11435.
(64) Brückner, S.; Allegra, G.; Corradini, P. *Macromolecules* **2002**, *35*, 3928.

MA0606758